Research Article

Propellants, Explosives, Pyrotechnics

doi.org/10.1002/prep.202100196

Validation of CL-20-based Propellant Formulations for Photopolymerization 3D Printing

Yuchen Gao,[a] Weitao Yang,*[a, b] Rui Hu,[a] Jing Zhou,[a] and Yucheng Zhang[a]

Abstract: The combustion performances of propellants depend on the geometry and the composition. Three-dimensional (3D) printing or additive manufacturing provides a feasible and effective way to fabricate propellants according to interior ballistic requirements. The main objective of this paper is to improve the properties of 3D printed propellants in terms of energy content and combustion behavior. Three propellant formulas, which contain polyurethane-acrylic acid resin as binder and hexanitrohexaazaisowurtzitane (CL-20) as energetic filler, were fabricated by extrusion material 3D printing. The formulas with the force constant of 1107.43–1209.44 J/g were designed. The combustion behaviors of designed formulas, such as the maximum pressure, burn time, and burn rate, were characterized by closed bomb tests. Meanwhile, the curing time, printability, and inner structure of these formulas were also demonstrated to understand the 3D extrusion printing of propellants better.

Keywords: Gun Propellants · 3D Printing · Photopolymerization · Combustion performance

1 Introduction

Propellants are the energy source for propelling a projectile or rocket by the expansion of combustion gases [1]. The gas generation rate is connected with the geometries of propellants, which are mainly determined by fabrication techniques. 3D printing (also known as additive manufacturing) provides a method to fabricate objects from 3D models according to the layer-by-layer principle. Thus, complex propellant geometries with better combustion performances can be easily fabricated by 3D printing [2].

Material Extrusion 3D printing is a familiar additive manufacturing process in which material is selectively dispensed through a nozzle or orifice on a platform [3]. The significant advantage of this method is the applicability for printing slurries with high viscosity or high solid content [4]. Compared with Fused Deposition Modelling (FDM), it is better to extrude propellant materials at near room temperature conditions for safety consideration. Thus, two energetic slurries have been developed for 3D Material Extrusion used in propellants, i.e., nitrocellulose-based solution and photocurable composite slurries [2]. Primarily, researchers focus on the 3D printing of nitrocellulose solutions. Sun [5] used ethyl acetate to solve nitrocellulose (NC)/nitro-glycerine (NG) carpet for 3D printing. The optimal concentration is about 45 %. Zhou [6] solved an NC-based formulation (50 wt.% NC, 20 wt.% NG, 10 wt.% diethylene glycol dinitrate (DEGDN), and 20 wt.% RDX) with alcohol/ketone solvent, the concentration is 25–50 wt.%. The drawback of these slurries is that the solvent needs to be removed after printing, introducing printing precision and efficiency problems.

Alternative slurries for 3D printing are the developed curable composite formulas [7,8]. The slurry can be cured in seconds under the radiation of ultraviolet (UV) light. McClain [9] and Chandru [4] studied the extrusion 3D printing of composites rocket propellants composed of photocurable resin and Ammonium perchlorate (AP). These kinds of slurries can print composite propellants with high solids loadings without the addition of solvents. For gun propellants, TNO developed RDX/acrylate-based compositions as used in co-extrusion 3D printing. The solid loads were 60 wt.% and 70 wt.%, respectively. The force constants of the two compositions were 713 J/g and 1032 J/g. The burn rates of samples varied from 2.4 cm/s to 13.1 cm/s at 200 MPa [8]. Thus, the photocurable formulas used in previous research had low burn rates. It is imperative to develop printable photocurable gun propellant formulas.

In this paper, printable propellant formulas with high energy were designed and printed by 3D Material Extrusion technology. A typical high energy density compound, CL-20, was used as the energetic filler to improve energy content and burn rate. The curing rate, printability, inner morphology, and combustion performances were studied and demonstrated.

[a] *Y. Gao, W. Yang, R. Hu, J. Zhou, Y. Zhang*
Xi'an Modern Chemistry Research Institute
Xi'an, 710065, P. R. China
**e-mail: njyangweitao@163.com*
[b] *W. Yang*
Xi'an Jiaotong University
Xi'an, 710049, P. R. China

2 Experimental Section

2.1 Materials and Formulations

Propellant formulas are composed of CL-20, polyurethane-acrylic acid resin, and diphenyl-(2,4,6-trimethyl benzoyl)-phosphine oxide (TPO). ε-CL-20 (50 μm) is provided by Liaoning Qingyang Chemical Co. Ltd. Polyurethane-acrylic acid resin (APU) is composed of polyurethane-acrylic acid resin and TPO. The viscosity of the binder matrix is 15.9 Pa·s. TPO acts as the photoinitiator with the content of 2 wt.%.

Figure 1 presents the force constant (*f*) and flame temperature (T_v) of formulas with 70 wt.%, 75 wt.%, and 80 wt.% CL-20, calculated by EMTRIX software. The force constants of formulas are 1107.43 J/g, 1152.73 J/g, and 1209.44 J/g, respectively. The flame temperatures of samples are 2895.5 K, 3001.44 K, and 3148.0 K, respectively. These thermal-chemical parameters are similar to that of triple-based propellants [10].

2.2 Photocuring Time Test

An LT-631 High-Speed Dielectric Cure Monitor (Lambiet Technologies, LLC, United States) was used to monitor the curing process [11]. The propellant slurry was deposited on the surface of the sensor under the radiation of UV light. The power of the UV light was 100 mW. The test temperature was about 293.1 K. The log ion viscosity-curing time (*t*) curves were measured.

The degree of curing has a correlation with the UV exposure time (*t*), which can be calculated by the ion viscosity. According to the application of dielectric analysis for monitoring the curing process [12], the degree of curing $\alpha(t)$ can be represented as a function of UV light irradiation time (*t*) according to Equation (1):

$$\alpha(t) = (\log\eta_t - \log\eta_0)/(\log\eta_\infty - \log\eta_0) \quad (1)$$

Where η_0 is the initial ionic viscosity of the propellant slurry; η_t is the ionic viscosity at time *t*; η_∞ is the maximum ionic viscosity.

2.3 Preparation of Samples

A self-developed 3D Material Extrusion Printer was used to print propellant samples. The schematic diagram of the 3D Material Extrusion Printer was as shown in Figure 2. The 3D printer consists of three modules:

(1) Three-axis moving platform for realizing three degrees of freedom of movement;
(2) Material extrusion module for extruding slurries at a certain speed;
(3) UV light laser module for curing the extruded lines.

All designed formulations were mixed in a slurry mixer for 1 hour. Then, the slurries were extruded through a 1 mm nozzle at the speed of 250 mm/min. The extruded lines were dispensed layer by layer on the platform according to preset paths. To prevent the collapse of the deposits and guarantee fast curing, two UV lasers (100 mW) focused on the extruded lines. The photographs of demonstrating samples were shown in Figure 3.

The Scanning Electron Microscope (SEM, FEI Quanta 600F, United States) was used to observe the internal morphology of propellants with high solid loadings. The distribution of CL-20 will affect the combustion stability of propellants. Moreover, the interface between solid and matrix will affect mechanical properties. Therefore, the distribution and interface can be studied by observing the internal morphology of the samples.

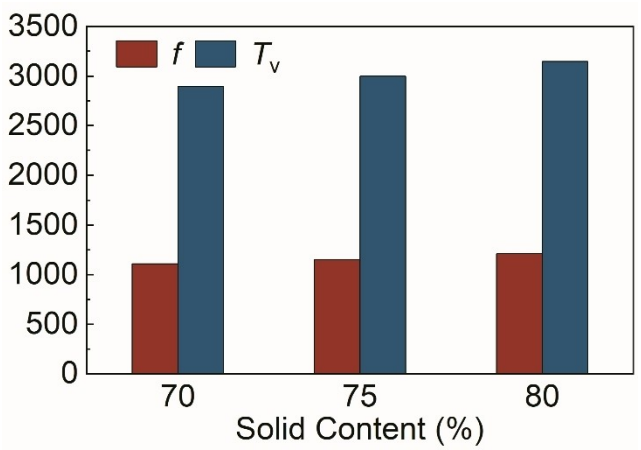

Figure 1. Results of thermodynamic calculations for designed formulas.

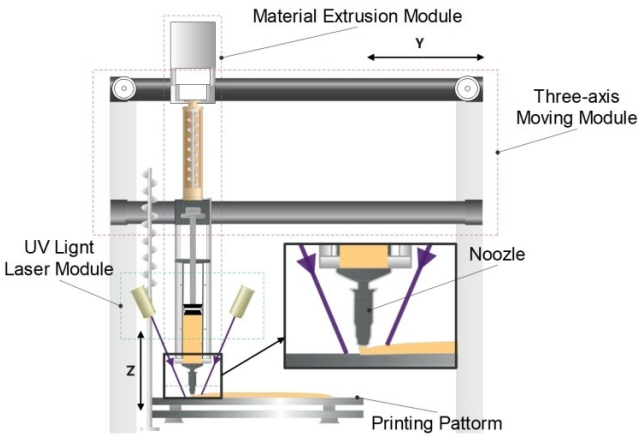

Figure 2. Schematic diagram of the 3D material extrusion printer.

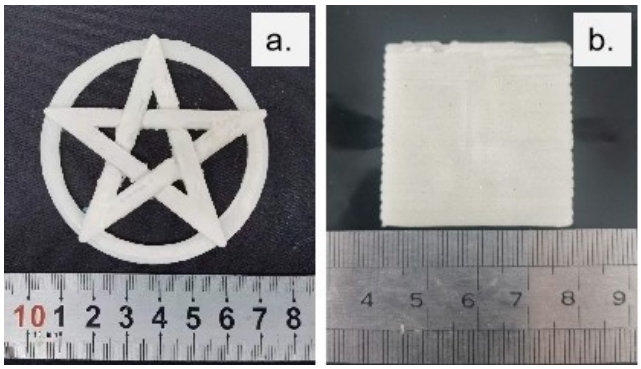

Figure 3. Photographs of printed complex sample (a) and sheet sample (b).

2.4 Combustion Diagnostics

The combustion properties were investigated by a closed bomb with a volume of 106 mL at a loading density of 0.20 g/cm^3. The samples were ignited by Numb.2 nitrocellulose (N% = 12.4%). The tested samples were 10× 10 mm slices chopped from sheet samples shown in Figure 3b. The thickness was 2.5 mm.

The pressure histories were obtained by a pressure sensor and a data acquisition system. The burn rate (u) was obtained by the fundamental burn rate equation of Vieille, as shown in Equation (2).

$$u = u_1 \cdot p^n \quad (2)$$

Where u_1 is the burn rate coefficient, and n is the pressure exponent, p is the pressure at time t.

3 Results and Discussion

3.1 Curing Dynamic Analysis

The curing time and curing degree are essential parameters of the curing process. Dielectric Analysis is one of the most frequently used in-process measurements for monitoring the cure of polymer binders [13]. The ion activity is expressed through dielectric analysis by the value of ionic viscosity, which reflects the degree of curing in the 3D printing process [12].

The ion viscosity change was shown in Figure 4. The ion viscosity in slurries increased rapidly once exposed to UV light. After several seconds, the curing reaction was almost finished. The curing rates and the corresponding time calculated according to Equation (1) were shown in Table 1. As shown in Table 1, the pure resin needed only 3.66 s to reach a curing level of 50%. The addition of solid filler prevented the cure reaction of the active groups in the resin matrix, refracted, and reflected the UV laser, resulting in a long time for curing [11]. Thus, the composite slurries containing 70–80 wt.% solid fillers need about 12–19 s to cure 50%.

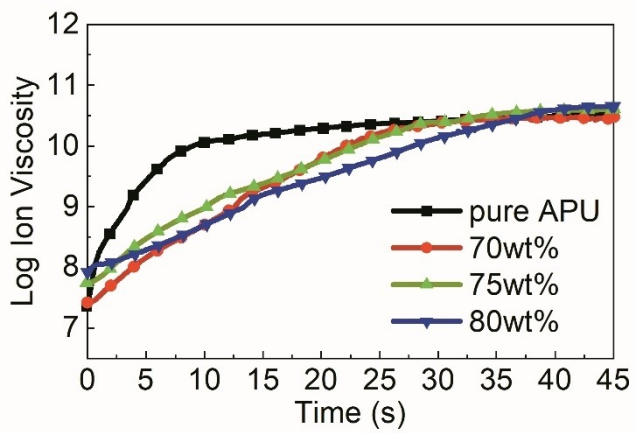

Figure 4. Effect of CL-20 content on UV curing.

Table 1. Relationship of curing degrees with time for samples with different contents.

Sample	$t_{25\%}$ (s)	$t_{50\%}$ (s)	$t_{75\%}$ (s)	$t_{\geq 90\%}$ (s)
pure-APU	0.93	3.66	8.60	≥38.58
70 wt.%	5.33	12.54	19.73	≥25.54
75 wt.%	5.77	15.10	26.05	≥68.30
80 wt.%	9.78	18.96	30.54	≥40.56

3.2 Internal Morphology

The Scanning Electron Microscope was used to observe the internal morphology of samples, as shown in Figure 5. CL-20 crystals were observed with no matrix cracking in Figure 5. The interface of CL-20 crystals and binder was firmly bound. After liquid nitrogen brittle fracture, energetic crystals were still embedded in the matrix with transcrystalline fracture. No dimples were observed in images, and the crystal fracture showed brittle fracture characteristics with typical cleavage fracture characteristics. It can be observed that the distribution density of Cl-20 crystals gradually increased with the increase of solid contents.

3.3 Combustion Performance

To evaluate the burning performance of propellants, closed bomb tests were conducted. p-t and u-p curves of samples were shown in Figure 6. The feature points were listed in Table 2. As shown in Figure 6a, with the increase of CL-20 content, the combustion time decreased from 18.44 ms to 8.32 ms, shorter than previous formulas (142.98 ms) [14]. The maximum pressures were 241.46 Mpa–289.44 MPa, in-

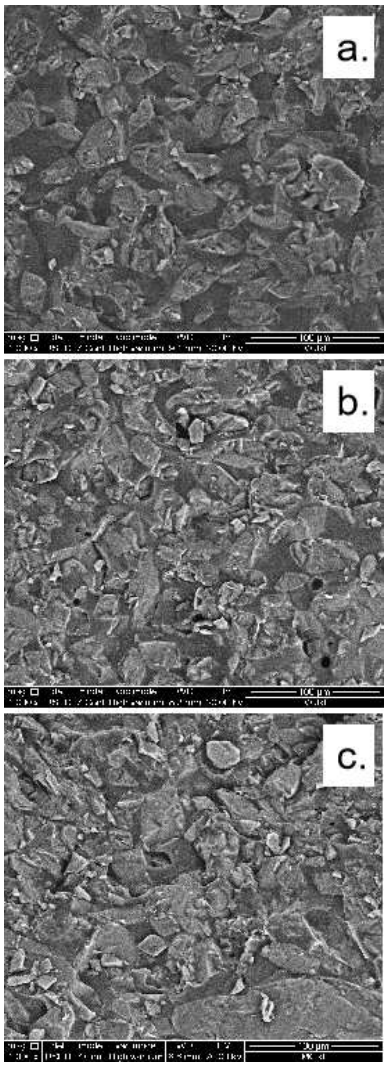

Figure 5. SEM image of samples with 70 wt.% (a), 75 wt.% (b), and 80 wt.% (c) CL-20.

dicating an increase in maximum pressure by 45.9–74.9% compared with previous formulas [14].

As shown in Figure 6b and Table 2, the burn rate increased from 11.88 cm/s to 18.59 cm/s at 100 MPa, with the solid content increasing. In the previous studies [7,14], the burn rates of printed propellants were less than 5 cm/s at 100 MPa, and the burn rate of a traditional triple-base propellant is about 10 cm/s [14]. The combustion performance of designed propellants was improved in terms of burn rate. However, the pressure exponents of formulas were 1.35, 1.27, and 1.41, respectively, which were too high to more than 1. The high-pressure exponent may lead to safety problems in the internal ballistic process [15]. This drawback may be solved in further studies.

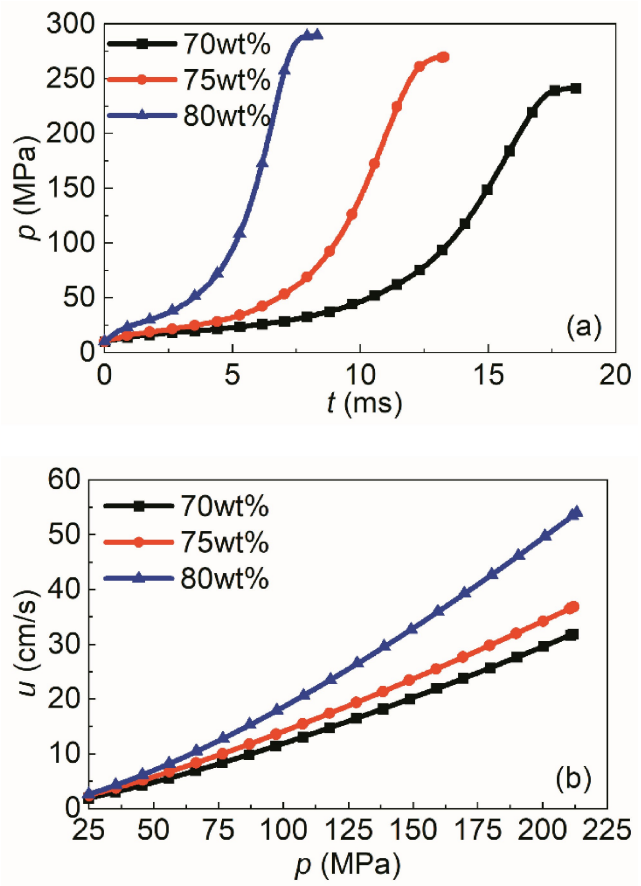

Figure 6. *p–t* curves (a) and *u–p* curves (b) of CL-20-based propellants.

Table 2. Combustion characteristic parameters.

Solid Content	*t* (ms)	*n*	*u* (cm s^{-1})		
			100 MPa	150 MPa	200 MPa
70 wt.%	18.44	1.35	11.88	20.26	29.55
75 wt.%	13.28	1.27	14.10	23.66	34.17
80 wt.%	8.32	1.41	18.59	32.89	49.39

3.4 Combustion Performances under Various Ignition Pressures

Ignition affects the combustion performance of propellants as the starting condition of propellant combustion [16]. The propellants were ignited by 1.1 g and 1.5 g NC powder. The ignition pressure was 10 MPa and 13.6 MPa, respectively. Figure 7 presented the effect of ignition pressure on *p-t* and *u-p* curves of propellant containing 70 wt.% CL-20. With the increase of ignition pressure, the combustion time decreased from 18.44 s to 16.84 s. Nevertheless, burn rates were approximate at the same pressure.

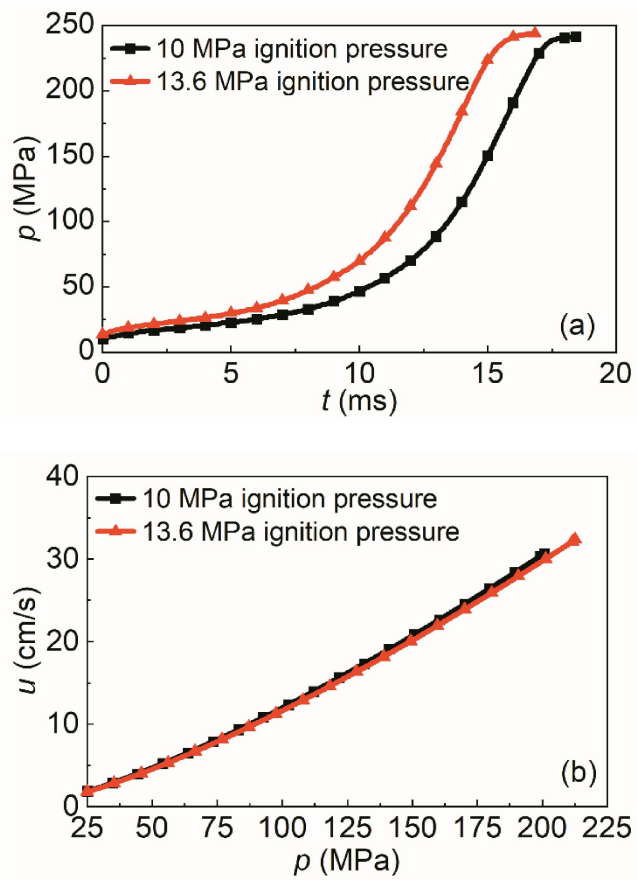

Figure 7. *p–t* curves (a) and *u–p* curves (b) of samples at different ignition pressures.

4 Conclusion

In this paper, three CL-20-based formulas were designed. Their combustion performance was studied by close bomb tests. Compared with the previous formulas, the designed CL-20-based formulas have higher force constants. The force constant of designed formulations was increased by more than 27 %. The burn rate of CL-20-based propellants varies from 11.88 cm/s to 18.59 cm/s at 100 MPa, with the solid content increasing. The burn rate was increased by more than four times. However, the pressure exponent of designed formulas is still too high. Therefore, CL-20-based photocurable formulas should be further optimized for decrease pressure exponent.

Data Availability Statement

The data that support the findings of this study are available from the corresponding author upon reasonable request.

References

[1] J. P. Agrawal, High Energy Materials: Propellants, Explosives, and Pyrotechnics, *John Wiley & Sons*, **2015**, p. 218.
[2] W. T. Yang, X. Xiao, R. Hu, J. X. Yang, Y. H. Zhao, Q. L. Wang, Developments of Additive Manufacture Technology in Propellants, Explosives and Pyrotechnics, *Chin. J. Explos. Propellants* **2020**, *43*, 1–11.
[3] S. Wickramasinghe, T. Do, P. Tran, FDM-Based 3D Printing of Polymer and Associated Composite: A Review on Mechanical Properties, Defects, and Treatments, *Polymers* **2020**, *12*, 1529.
[4] R. A. Chandru, N. Balasubramanian, C. Oommen, B. N. Raghunandan, Additive Manufacturing of Solid Rocket Propellant Grains, *J. Propul. Power* **2018**, *34*, 1090–1093.
[5] Y. L. Sun, Study on Process Adaptability of Energetic Material in Additive Manufacturing by Solvent Method, *Nanjing: Nanjing University of Science & Technology* **2017**.
[6] M. L. Zhou, F. Q. Nan, W. D. He, M. R. Wang, Design and Preparation of Propellant 3D Printer Based on Extrusion Deposition Technology, *Chin. J. Energet. Mater.* **2021**, *29*, 530–534.
[7] M. H. Straathof, C. A. van Driel, J. N. J. van Lingen, B. L. J. Ingenhut, A. T. ten Cate, H. H. Maalderink, Development of Propellant Compositions for Vat Photopolymerization Additive Manufacturing, *Propellants Explos. Pyrotech.* **2020**, *45*, 36–52.
[8] M. Straathof, C. van Driel, A. den Otter, J. van Lingen, J. Heinsius, J. Isenia, B. Rijnders, Gradient Printing of Energetic Materials – First Results, *31st International Symposium on Ballistics*. Hyderabad, India, November 4–8, **2019**, p. 62–74.
[9] M. S. McClain, I. E. Gunduz, S. F. Son, Additive Manufacturing of Ammonium Perchlorate Composite Propellant with High Solids Loadings, *Proc. Combust. Inst.* **2019**, *37*, 3135–3142.
[10] B. Vogelsanger, A. Huber, H. Jaskolka, Insensitive Propulsion Systems for Large Caliber Ammunition, *Insensitive Munitions, and Energetic Materials Technology Symposium*, Miami, Florida, USA, October 15–17, **2007**, p. 3.
[11] Z. H. Yu, A. Y. Cui, P. Z. Zhao, H. K. Wei, F. Y. Hu, Preparation and Properties Studies of UV-Curable Silicone Modified Epoxy Resin Composite System, *J. Appl. Biomater.* **2018**, *16*, 170–176.
[12] M. Sernek, F. A. Kamke, Application of Dielectric Analysis for Monitoring the Cure Process of Phenol-Formaldehyde Adhesive, *Int. J. Adhes. Adhes.* **2007**, *27*, 562–567.
[13] C. E. Frazier, Monitoring Resin Cure in the Mat for Hot-Compression Modelling, *Fundamentals of Composite Processing: Proceedings of a Workshop*, Madison, Wisconsin, USA, November 5–6, **2003**, p. 26–28.
[14] W. T. Yang, R. Hu, L. Zheng, G. H. Yan, W. R. Yan, Fabrication and Investigation of 3D-Printed Gun Propellants, *Mater. Des.* **2020**, *192*, 8.
[15] Y. Zhao, L. X. Yang, Y. Liu, H. L. Zhao, J. W. Jin, L. D. Liu, B. M. Zhao, Z. Z. Zhang, Effect of Particle Size and Types of Nitramines on Combustion Performance of ETPE Gun Propellants Based on BAMO-AMMO, *Chin. J. Energet. Mater.* **2010**, *18*, 397–401.
[16] L. J. Chao, B. F. Lv, Effect of Changing Ignition Dosages on Combustion Properties of Propellants, *J. Ordnance Equip. Eng.* **2016**, *37*, 126–128.

Manuscript received: July 4, 2021
Revised manuscript received: August 16, 2021
Version of record online: October 14, 2021